

Article

Comparing the Air Turbulence above Smooth and Rough Surfaces in the Amazon Region

Raoni A. S. Santana¹, Cléo Q. Dias-Júnior^{2,*}, Roseilson S. do Vale¹, Júlio Tóta¹, Rodrigo da Silva¹, Raphael Tapajós¹, Antônio O. Manzi³ and Troy P. Beldini⁴

- ¹ Institute of Engineering and Geosciences, Federal University of Western Para (UFOPA), Santarém 68040-255, PA, Brazil; raoni.santana@ufopa.edu.br (R.A.S.S.); roseilson.vale@ufopa.edu.br (R.S.d.V.); totaju@gmail.com (J.T.); rodrigo.silva@ufopa.edu.br (R.d.S.); rpablotapajos@gmail.com (R.T.)
- ² Department of Physics, Federal Institute of Pará (IFPA), Belém 66093-020, PA, Brazil
- ³ National Institute for Space Research (INPE), São José dos Campos 12630-000, SP, Brazil; antonio.manzi@inpe.br
- ⁴ Institute of Biodiversity and Forests, Federal University of Western Para (UFOPA), Santarém 68040-255, PA, Brazil; tpbeldini@yahoo.com
- * Correspondence: cleo.quaresma@ifpa.edu.br

Abstract: The goal of this work is to compare the main air turbulence characteristics of two common areas in the Amazonian landscape: a dense forest (rough surface) and a water surface (smooth surface). Using wind components data collected at high frequency by sonic anemometers located just above these surfaces, turbulence intensity and power spectra, temporal and length scales of the eddies, as well as the main terms of the TKE budget (TKE = turbulent kinetic energy) were evaluated for each surface type. The results showed that in general, the air turbulence intensity above the forest was higher than above the lake during the daytime, due to the high efficiency of the forest in absorbing the momentum of the turbulent flow. During the nighttime, the situation was reversed, with greater air turbulence intensity above the lake, except in some periods in which intermittent turbulence bursts occurred above the forest.

Keywords: amazon forest; smooth and rough surfaces; TKE budget; turbulence



Citation: Santana, R.A.S.; Dias-Júnior, C.Q.; do Vale, R.S.; Tóta, J.; da Silva, R.; Tapajós, R.; Manzi, A.O.; Beldini, T.P. Comparing the Air Turbulence above Smooth and Rough Surfaces in the Amazon Region. *Atmosphere* **2021**, *12*, 1043. <https://doi.org/10.3390/atmos12081043>

Academic Editors: Qiusheng Li, Junyi He and Bin Lu

Received: 21 June 2021
Accepted: 11 August 2021
Published: 14 August 2021

Publisher's Note: MDPI stays neutral with regard to jurisdictional claims in published maps and institutional affiliations.



Copyright: © 2021 by the authors. Licensee MDPI, Basel, Switzerland. This article is an open access article distributed under the terms and conditions of the Creative Commons Attribution (CC BY) license (<https://creativecommons.org/licenses/by/4.0/>).

1. Introduction

It is known that the structure of atmospheric turbulence in the surface boundary layer will depend on the degree of surface roughness [1]. In the Amazon, surface roughness is quite heterogeneous, since, in addition to the presence of the exuberant densely forested lands, the presence of aquatic environments is very common, and there is great diversity of these ecosystems, such as flooded forests, floodplains, igapós (blackwater flooded forests that remain flooded even during the dry season), and open and closed fields. The region, during the high-water period (May–June), has a flooded area of 350,000 Km², or about 20% of the volume of the mainstream Amazon River [2].

It is assumed that for different Amazonian soil types there will be different processes of turbulent exchanges between the surface and the atmosphere [3,4]. In addition, it is known that turbulence processes in the atmospheric surface layer play a major role in the transport of momentum, sensible and latent heat fluxes [5], particularly in the surface layer where the turbulent fluxes are essential for mediating the interactions between the atmosphere and surface.

Although the turbulent structures in horizontally homogeneous surface layers are well known [6], for rough surfaces, as is the case of the Amazonian forest, a better understanding of such structures is still needed. Research on this subject has been conducted for over 30 years in the Amazon region [7–13], but there are practically no studies that attempt to understand the structure of turbulence above water surfaces such as lakes in this region [14]. Such lakes have the peculiarity of being frequently surrounded by primary forests.

Turbulent flow power spectra are an important tool for determining the spatial and time scales of the component eddies [15,16]. The spectra at the top of the canopy differ from the spectra found at surface due to wake and wave effects over the canopy [17]. Studies show that the spectral curves are more peaked above the forest than in a canonical spectrum, possibly indicating that some variance is being lost due to the interaction of the wind flow with the canopy for frequencies in the inertial sub-range [18–20]. Fitzjarrald et al. [7] observed the $-2/3$ inertial sub-range above and within the upper half (region between $h/2$ and h , where h is the top of the canopy) of the Amazon forest canopy. In the lower canopy (region between $h/2$ and the forest floor) the spectra showed a relative deficit of power at mid-frequencies and an excess at the highest frequencies without showing a clear decay of $-2/3$ [8].

Above lakes, there are few studies that have reported how atmospheric turbulence is organized, and this is the case even for non-tropical regions. Studies of Sahlee et al. [21] taken at a Swedish lake show that the turbulence structure was highly influenced by the surrounding land during daytime and the variance spectra of both horizontal velocity and scalars during both unstable and stable stratification displayed a low frequency peak. Turbulence spectra obtained from water side measurements from ADV (Acoustic Doppler Velocimeter) in a shallow estuary followed the general shape of the curves and turbulent power laws [22], however, the curves were all shifted toward higher frequencies and showed spectral lag effects [23].

The goal of this work was to compare the main characteristics of the air turbulence of two common areas in the Amazonian landscape: a dense forest (rough surface) and a water surface (smooth surface). Using data from wind components collected at high frequency, turbulence intensity and power spectra, temporal and length scales of the eddies, as well as the main terms of the turbulent kinetic energy (TKE) budget were evaluated for each surface type. These areas contribute significantly to the total energy, mass and momentum budget in this region. The differences highlighted in this study are very useful for modeling processes involving parameterizations above surfaces with different roughness in the Amazon region.

2. Materials and Methods

2.1. Study Area

The data were collected at two sites located in the Brazilian Amazon. The first site was K34 located in the Cuieiras Biological Reserve - Manaus (AM) and the second at the Curuá-Una Hydroelectric Power Plant located in Santarém (PA) (Figure 1). The Cuieiras Biological Reserve is located in the Rio Negro Environmental Preservation Area – south sector. Cuieiras is approximately 80 km North of Manaus and comprises about 10 thousand ha ($02^{\circ}36'33''$ S and $60^{\circ}12'33''$ W) [24]. It is an undisturbed area with primary lowland vegetation and is in the Igarapé Asu watershed. This area is reserved for ecological, botanical and meteorological surveys. The Curuá-Una dam is located in the Lower Amazon River Basin ($41,531.51$ km²) in the Curuá-Una River, at the waterfall Palhão ($02^{\circ}50'00''$ S and $54^{\circ}18'00''$ W), 70 km southeast of Santarém, in Pará State. The Curuá-Una hydropower plant was the second to be built in the Amazon and the reservoir was filled in 1977, occupying an area of 72 km² at the operational level, has 30.3 MW capacity, and is 68 m above sea level [25].

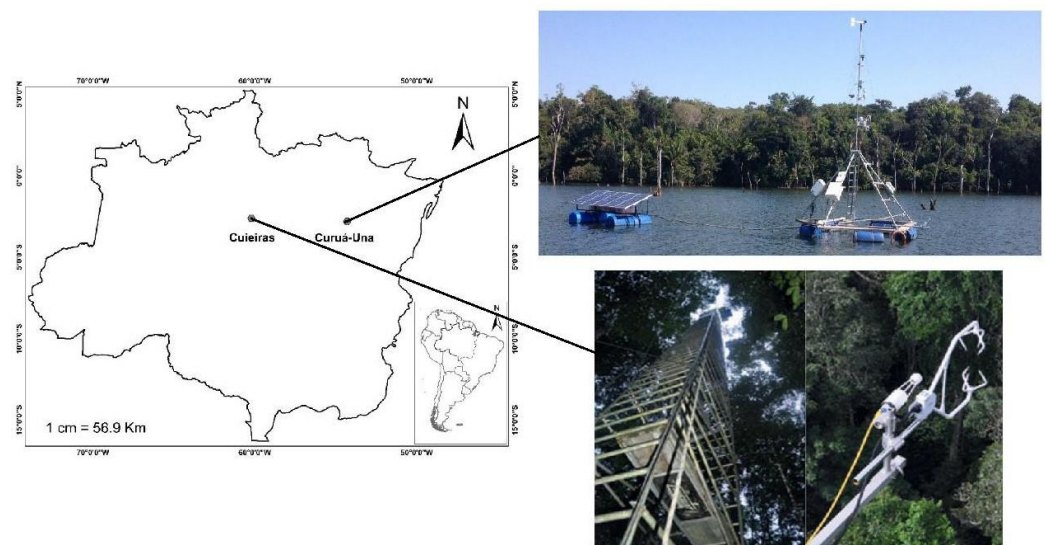


Figure 1. Map with the location of two study sites: Cuieiras (dense forest) near Manaus (AM) and Curuá-Una (lake) near Santarém (PA), both located in the Amazon region.

2.2. Data

At the K34 site, 10 three-dimensional sonic anemometers (CSAT3 model, Campbell Scientific Inc., Logan, UT, USA) were installed at 1.5, 7, 13.5, 18.4, 22.1, 24.5, 31.6, 34.9, 40.4 and 48.2 m above the ground during the period from April 2014 to January 2015, as part of the GoAmazon project [26]. The data used in this work corresponds to the three highest sonic anemometers. The wind components and the virtual sonic temperature data were collected at a rate of 20 Hz.

Data from the Curuá-Una (CU) site were collected during June 2015 to June 2016 from a floating micrometeorological platform with a shape of a regular pentagon, four anchor points, and a nearby floating power supply platform [14]. This platform was equipped with high and low frequency sensors for both water and air measurements. In this study we used data from the high frequency system (10 Hz) to measure the flux (open path EC 150—Campbell Scientific, Inc.). The system consists of a gas analyzer that measures the absolute densities of CO_2 and H_2O , a sonic anemometer (CSAT3A—Campbell Scientific, Inc.), which measures the orthogonal components of the wind and the sonic temperature. The system is 3 m above the surface of the water. Complementarily, data from 2 two-dimensional sonic anemometers (WindSonic, Gill Instruments Ltd., Lymington, UK), which provide wind speed and direction at a rate of 4 Hz, were used. These anemometers were installed at 1.5 and 4.5 m on the floating buoy structure.

2.3. Data Quality Control and Methodology

From the available data, 4 days from each site were chosen: 13–16 September 2014 for the K34 site and 15–18 September 2015 for the CU site. The objective was to find consecutive days where there was no interruption for an external reason (lack of power, for example) and also days with similar atmospheric conditions (no rain and low cloud cover). Once selected, the raw data were subjected to a tilt correction by the planar-fit method [27], as well as the removal of spikes according to [28].

To describe the atmospheric turbulent flow at the K34 and CU sites, data were calculated in intervals of 30 min, and the following equations were used: the wind speed $U = \sqrt{u^2 + v^2}$, where u and v are the zonal and meridional wind components, respectively; the vertical velocity (w) standard deviation, $\sigma_w = \sqrt{(\overline{w'})^2}$, friction velocity, $u_* = [(\overline{u'w'})^2 + (\overline{v'w'})^2]^{1/4}$, sensible heat flux, $H = \rho c_p \overline{w'\theta'_V}$, where ρ is the air density, c_p is the air specific heat of dry air at constant pressure; θ'_V is the virtual potential temperature; and the prime symbol indicates the variable value minus its mean. The drag coefficient,

$C_D = u_*^2 / U^2$ [29,30]; and Monin-Obukhov stability parameter, z/L , where z is the height and L is the Obukhov length, defined as:

$$L = \frac{-\theta_V u_*^3}{kgw'\theta'_V} \tag{1}$$

where k is the von Karman constant (we assume $k = 0.4$) and g is the gravity acceleration. In addition, other variables described below were measured.

The linear correlation coefficient between any two variables was calculated as:

$$r_{AB} = \frac{\overline{A'B'}}{\sigma_A \sigma_B} \tag{2}$$

In our case $A = w$ and $B = u; T$, where T is the air temperature. From this point forward u was align with the mean wind vector [27]

The horizontal (Λ_u) and vertical (Λ_w) integral scales of the largest eddies were also calculated, based on the u and w correlograms, respectively. Figure 2 shows an example of how such scales were obtained after obtaining the autocorrelation according to Equation (3) (which is derived from Equation (2)):

$$r_x(\xi) = \frac{\overline{x'(t)x'(t+\xi)}}{\sigma_x^2} \tag{3}$$

where $x = u, w$; ξ is the time lag with respect to time, and the values of the integral scales will be numerically equal to the area under the curve in the interval between $t = 0$ and t for the first r root, i.e., where the curve touches the abscissa axis for the first time [16,17].

Therefore,

$$\Lambda_x = \int_0^\infty r_x(\xi) d\xi \tag{4}$$

Using the Taylor hypothesis we obtained the length scales of the largest eddies, $L_x = U\Lambda_x$.

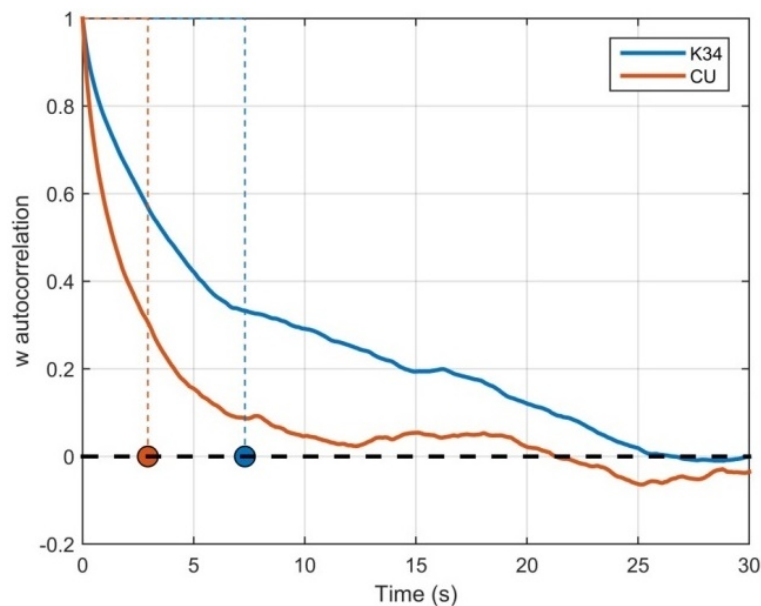


Figure 2. Vertical velocity correlogram. Autocorrelation was calculated for 30 min of data from each site with a time lag every second. The circles represent the Λ_w values for both CU (red) and K34 (blue) sites. Such values are numerically equal to the areas formed under the curves of each site.

Using the fast Fourier transform (FFT) the w power spectra of the wind vertical (S_w) and horizontal (S_u) velocities were obtained. From S_u and assuming the applicability of the Taylor's hypothesis as well as the spectral properties established by Kolmogorov, the TKE dissipation rate was calculated according to the equation:

$$\epsilon = \frac{2\pi f^{5/2} S_u^{3/2}}{U \alpha^{3/2}} \quad (5)$$

where f is the frequency; S_u is the u power spectra; and $\alpha = 0.55$ is Kolmogorov's constant [17,22]. In order to select only values of S_u that were inside the inertial subrange, we used values of the frequency range $1.0 < f < 2.5$ Hz [10,31].

In addition to ϵ , two other TKE budget equation terms were calculated: buoyancy, $(g/\theta_V)\overline{\theta'_V w'}$, and wind shear production, $(\overline{u'w'})\frac{\partial U}{\partial z}$, where z is the height.

3. Results and Discussion

In general the turbulence intensity in the atmospheric boundary layer (ABL) presents its highest values close to the surface [15], since momentum is extracted from the flow at this surface. The results presented in Figure 3 show that the way the flow interacts with the surface differs greatly between the rough surface, above the K34 forest canopy, and the smooth surface, above the CU Lake. The figure also shows that the w values are higher during the day and lower at night (Figure 3a,b), in both investigated sites. The same behavior is observed for the horizontal wind speed (Figure 3c). The behaviors of the diurnal cycles of U and w are expected in ABL since they present low values during the night, due to the negative net radiation, and increase gradually during the day following the radiation diurnal cycle.

When comparing the w values for K34 and CU it is observed that they were higher above the forest during the day. However, during the night the behavior is reversed, except for some short periods where the w values above the forest were very high. This is characteristic of locations in the night phase of the ABL [10,11,32,33], including the Amazon rainforest [34]. The interesting result is that these turbulence bursts are not present above the lake, even when analyzing data from other nights not included in the current study.

The σ_w values, which are associated with the turbulence intensity, are shown in Figure 3d. It is observed that the σ_w values follow a similar trend to the w values, that is, above the forest, they were higher for the daytime when compared to the lake. During the night, although the turbulence intensity above the lake is weak, it is greater than above the forest, except in those moments of intermittent turbulence mentioned above. Far from these events the σ_w values were very close to zero above the forest during the nighttime period, but there was an increase of σ_w values above the lake as the night progressed. It is noted that the turbulence intensity is relatively high above the lake during the night-day transition, and this behavior will be better explained in the next sections.

The U cycles were quite regular and presented a behavior that was repeated over time with higher values during the daytime above the lake than over the forest canopy (Figure 3c). This occurred even though the measurement height of this variable on the lake was closer to the surface (3 m above CU surface and 5 m above the K34 canopy), and considering that the wind is expected to increase with height in the surface layer [17,35–37].

Figure 3e shows the u_* time series. The behavior of this variable shows that although the wind speed is higher above the lake during the day the u_* values are much higher over the forest in this period. This behavior may be related to the different capacities that each surface presents in absorbing momentum and producing wind shear from the atmospheric flow. During the night the u_* values are close to zero for both sites.

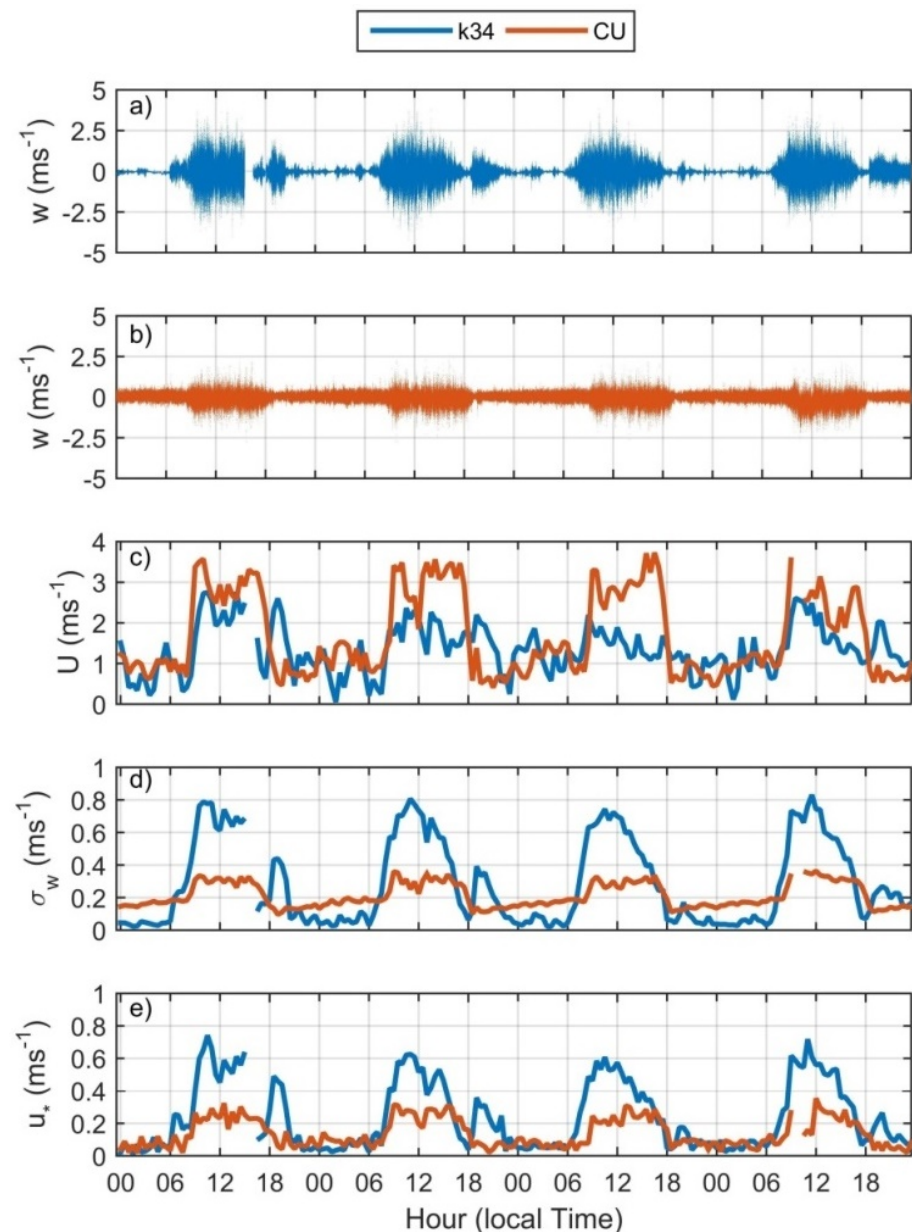


Figure 3. Time series of the w wind component (a,b), mean wind (c), w standard deviation (d) and friction velocity (e) for K34 (blue) and CU (red) sites. The variables shown in (a,b) are sampled at 20 and 10 Hz, respectively. The variables shown in (c–e) correspond a 30 min average.

It is worth remembering that an important property of the roughness sub-layer above the forest is the dependence of the organization of turbulence as a function of tree arrangement [17,38]. Forest heterogeneity influences canopy efficiency in absorbing momentum [31]. A good parameter for measuring the absorption rate of atmospheric momentum flow through the forest is the correlation coefficient r_{uw} . When r_{uw} has low values little TKE is being converted to momentum flow. In contrast, if r_{uw} has high values, then TKE is being transformed into momentum flux quite efficiently. The values of r_{wT} also indicate the efficiency of the TKE transformation, but now, into H . Low values of r_{wT} indicate low efficiency in transforming TKE into H and vice versa. Positive values of H and consequently r_{wT} indicate a heat flux whose direction is from the surface to the atmosphere, while negative values indicate the opposite direction.

Thus, it can be seen from Figure 4a that the values of r_{uw} (in modulus) were almost always higher above the forest than above the lake, that is, the forest is more efficient

in turning TKE into momentum flux. This result corroborates the higher values of u_* (momentum flux) above the forest (mainly during the day), where the horizontal wind speeds were lower than above the lake.

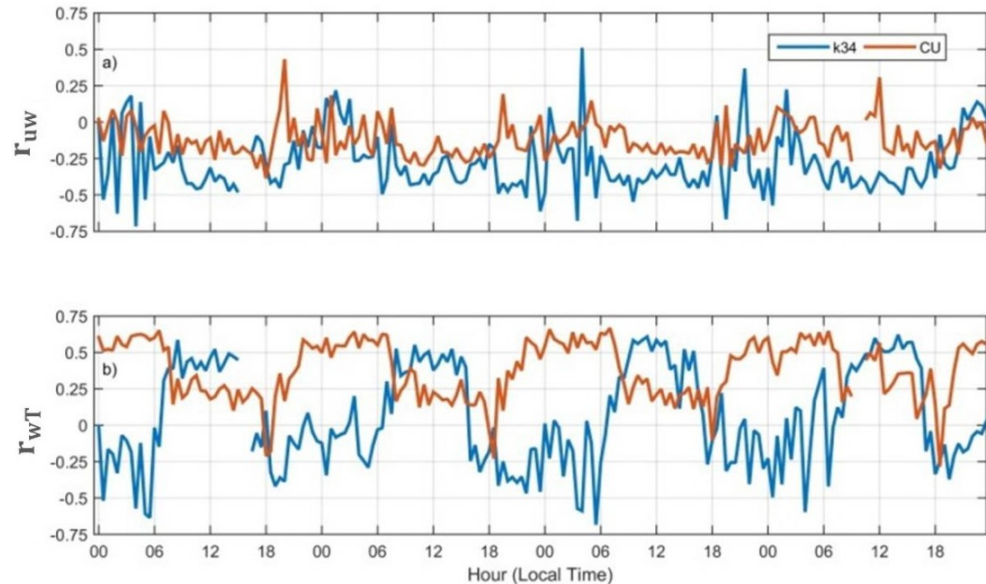


Figure 4. (a) Correlation coefficient between u and w and (b) correlation coefficient between w and T for K34 (blue) and CU (red) sites.

Figure 4b shows the correlation coefficient values between vertical wind speed and temperature (r_{wT}), and shows that the r_{wT} values above the lake were almost always positive (except for at 18 LT), unlike for the forest where they were positive during the day and negative at night. During the day the r_{wT} values were higher above the forest than above the lake, as a consequence there is a considerably larger turbulent sensible heat flux above the forest (Figure 5b). Over night times the behavior is exactly opposite, i.e., above the lake the values of r_{wT} (in module) are often higher than above forest and consequently the sensible heat flux above the lake is greater.

Figure 5 shows the daily average values of the Monin-Obukhov stability parameter (Figure 5a) and the sensible heat flux (H , Figure 5b) above the forest and lake. Overnight the z/L values show opposite signs above the lake and the forest. For the forest the z/L values were positive, indicating atmospheric stability, while for the lake z/L was negative, that is, the atmosphere on this surface is unstable. During the day the z/L values are negative and close to zero for both sites, indicating an atmospheric situation close to neutrality (mechanical turbulence in equilibrium with thermal turbulence).

The H values (Figure 5b) corroborate the z/L values, i.e., above the lake they are almost always positive (except at 18 LT), indicating that the lake was almost always warmer than the air above it. While above the forest H values are positive during the day and negative (close to zero) at night, as shown by several other studies [31,39]. One issue that draws attention to H above the forest is the increase in this flux from the atmosphere to the surface over time between 19–20 LT, the same time period for which intermittent turbulence was noted (Figure 3). We believe that such intermittent events have the ability to considerably increase sensible heat flux. According to Dias-Junior et al. [10] during episodes of intermittent turbulence in the Amazonian nocturnal boundary layer, the H values increased 5 times compared to the average values.

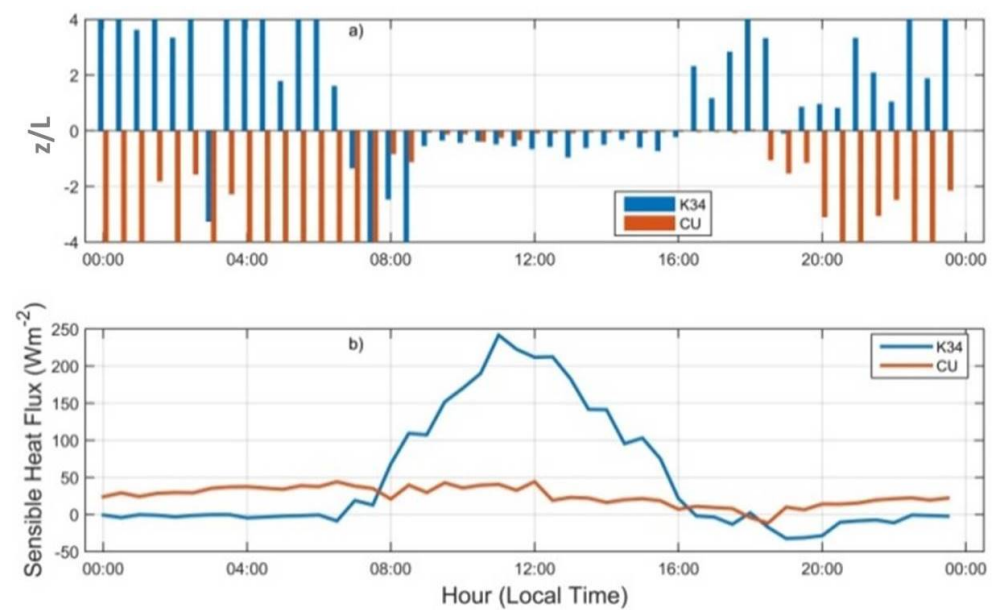


Figure 5. Diurnal cycle of the Monin-Obukhov Stability Parameter (a) sensible heat flux (b) for K34 (blue) and CU (red) sites.

Many parameterizations of atmospheric models or questions involving turbulence closure make it necessary to know the time and length scales of the eddies in the ABL, and Table 1 lists these scales which were calculated during the daytime and nighttime period at the K34 and CU sites. One variable that is used to precisely quantify surface drag in a fluid environment is the drag coefficient (c_D). This variable had values eight times higher above the forest than above the lake during the day, and two times higher during the night. In fact, the values of c_D above the lake are practically the same during the day and the night, unlike the c_D values above the forest, which drastically reduce when daytime values are compared with nighttime values. Since $c_D = u_*^2/U^2$ it is noted that above the lake the u_* values decrease similarly to the decrease of the U values, but above the forest the decrease of u_* is greater than U from day to night.

The horizontal and vertical integral scales of the wind components were measured at a single point during a certain period of time in this study, and represent the time in these series needed to maintain a significant correlation with themselves [40,41]. The integral scales presented higher values at the forest than those observed at the lake for both daytime and nighttime conditions (see Table 1)

From the values of the time scales the length scales of eddies were obtained assuming the validity of Taylor's hypothesis, with the recognition that this hypothesis is not always valid for forest areas, where, for the standard deviation of the mean wind velocity (σ_u), the relation $\sigma_u < 0.5U$ is rarely observed. Shaw et al. [41], using a two-point measurement system with varying spatial separation, hence being independent of Taylor's hypothesis, showed that single-point calculations match those using the two-point measurement in the region $z/h = 2-3$ (where h is the canopy height).

The L_w values were higher for daytime than nighttime conditions, both above the lake and above the forest. In addition, the L_w values above the forest were higher than the values found above the lake, but the difference between them is relatively small. The L_u values also were higher for daytime than nighttime conditions, both above the lake and above the forest. However, during the day the L_u values were higher above the lake than above the forest, unlike that observed for L_w .

The values of L_w and L_u found in this work indicate that even though the lake has a lower surface roughness than the forest (Figure 3 and Table 1), and therefore less shear, eddies above it have relatively similar lengths to eddies that populate the forest region.

Table 1. Time and length scales of the turbulent flow in the atmospheric boundary layer for the K34 and CU site. The variables are: drag coefficient (C_D), integral scale of the horizontal (Λ_u) and vertical (Λ_w) component of the wind and length scale of the eddies for horizontal (L_u) and vertical wind component (L_w).

	K34-Daytime	CU-Daytime	K34-Nighttime	CU-Nighttime
C_D	0.08 ± 0.03	0.01 ± 0.005	0.02 ± 0.07	0.01 ± 0.007
Λ_u (s)	18.3 ± 15.6	16.6 ± 20.9	4.5 ± 15.0	2.9 ± 11.1
Λ_w (s)	6.0 ± 2.7	3.5 ± 2.4	6.1 ± 5.2	5.2 ± 3.5
L_u (m)	35.2 ± 28.2	48.0 ± 60.8	5.3 ± 17.3	2.3 ± 9.3
L_w (m)	11.1 ± 3.2	9.3 ± 5.4	5.2 ± 8.6	4.6 ± 2.6

So far we have not found studies showing L_u and L_w values above lakes. This must be related to the difficulty of making measurements using the eddy covariance technique over this surface [42]. Above the forest the L_u and L_w values found here were comparable to those found by [8] for forest canopy in the Amazon. Taking the average height of the forest canopy at K34 as 35 m [26], the values of these length scales fit the pattern observed by [43], who observed $L_u \approx h$ and $L_w \approx h/3$ just above the canopy, studying different canopies.

The time and length scales calculated above refer to scales of eddies [17,40]. However, the turbulent flow in the ABL encompasses different sized eddies, which distinctly contribute to total kinetic energy of the flow [15], and to the power spectrum in function of the frequency, which is a variable that describes such characteristics [15]. Figure 6 shows composites of the w power spectra for the K34 and CU sites obtained during the daytime and nighttime periods at each site. The behavior of these spectra present considerable differences between the sites and even between the periods studied in a given site.

It is well documented and consolidated in the literature that the spectra of the wind velocity components when plotted as a function of frequency have a linear decay region with a coefficient of $-5/3$, called Kolmogorov's five-third law of spectrums [6]. In this region, called inertial sub-range, energy is neither produced or dissipated but transferred to smaller and smaller scales [17]. At the K34 site this region is well defined during the daytime and starts at $f \approx 10^{-1.9} \approx 0.013$ Hz, thus continuing to higher frequencies (Figure 6a); in contrast, during the night period this decay only appears from $f > 1$ Hz (Figure 6b).

Moraes et al. [20] studying the turbulence spectra and co-spectra in two areas in the Amazon (one with forest and another deforested) observed that many of these spectra obtained in wind conditions lower than 1 ms^{-1} during the nighttime did not show the decay of $-5/3$ in the inertial sub-range. Kruijt et al. [8] found relative deficit of power at mid-frequencies and an excess at the highest frequencies under conditions of atmospheric stability above the canopy of two forest sites in the Amazon. During the 4 days of data chosen for the analyses of the present study, 50% of the time the wind speed was below 1 ms^{-1} during the nocturnal period (Figure 3c). As the result shown in Figure 6b is a composite with all periods of the night, the decay of $-5/3$ still appears in a region of high frequencies due to the contribution to the spectrum of periods in which wind speed exceeded 1 ms^{-1} . According to [20], in this condition the turbulence spectra presented canonical behavior, with decay of $-5/3$.

Unlike the forest, the spectra calculated above the lake showed the decay region during both daytime and nighttime. Moreover, the inertial sub-range of the night spectrum seems clearer than the daytime spectrum (Figure 6c,d). The behavior of these two spectra differs subtly in the region of low frequencies of the spectrum, evidencing the presence of larger eddies during the daytime period compared to the nocturnal period above the lake. The fact that the nighttime w spectrum above the lake resembles canonical behavior indicates that turbulence is well developed in this period, which does not occur in the forest in at least 50% of the nighttime period. An important fact which may help to explain this turbulence above the lake is that the atmosphere almost always has unstable conditions

or is close to neutrality over the CU lake (Figure 5), favoring the vertical mixing of the atmosphere above [14].

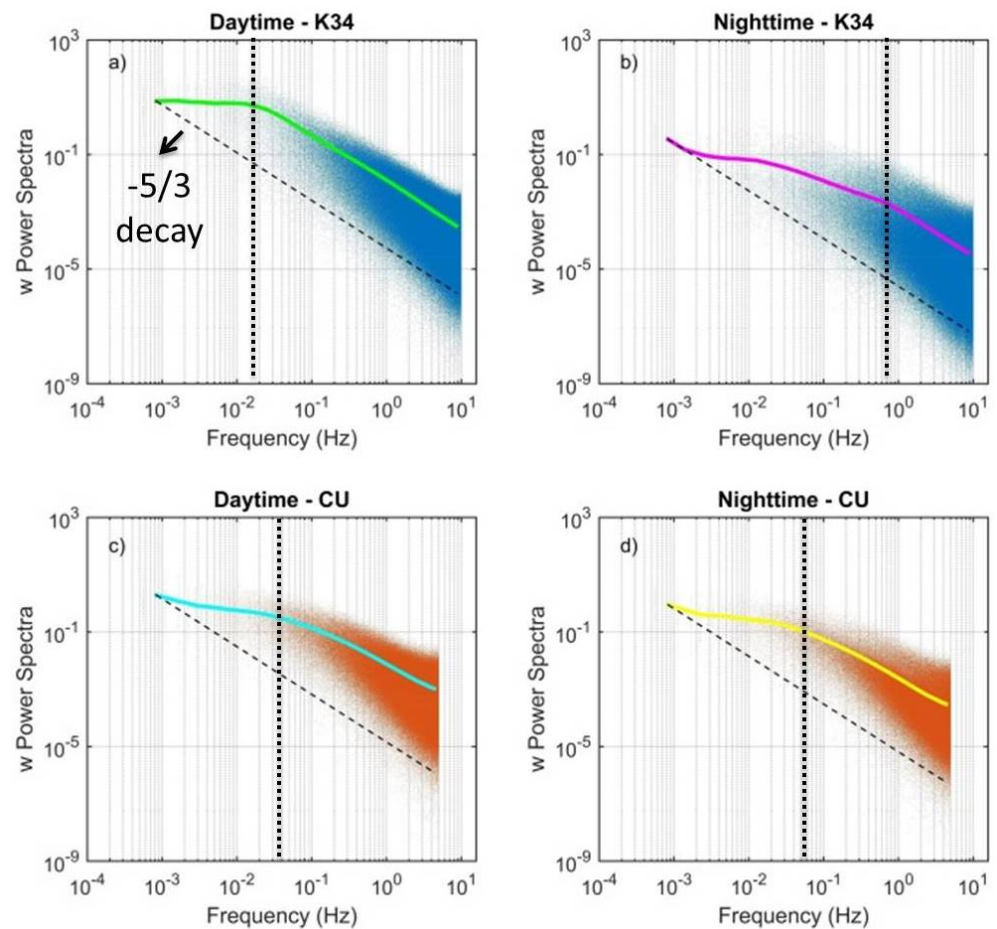


Figure 6. Power spectra of the vertical wind component at the K34 (a,b) and CU (c,d). The dotted vertical lines indicate the values of the frequency where the power spectrum starts to follow the $-5/3$ law.

An important question about the air turbulence on the surfaces studied in this work (smooth and rough) is to know how the terms of the TKE budget equation vary during their diurnal cycles. Figure 7 shows the cycles of buoyancy, shear production and TKE dissipation rate (ϵ), during the day and the night for the k34 (Figure 7a,b) and CU (Figure 7c,d) sites. For both forest and lake, shear production was greater than buoyancy during the daytime, a result expected for measurements very close to the surface. However, the possible explanation for the difference between these two terms at each site should be different. As previously seen, wind speed above the lake is higher than above the forest during the daytime, but as the surface is inefficient in absorbing momentum from the atmospheric flow this does not translate into greater turbulence intensity (Figure 3). Even so, shear production dominates during the day due to the lake's great thermal inertia. In the forest this occurs due to the high efficiency in absorbing momentum from the atmosphere.

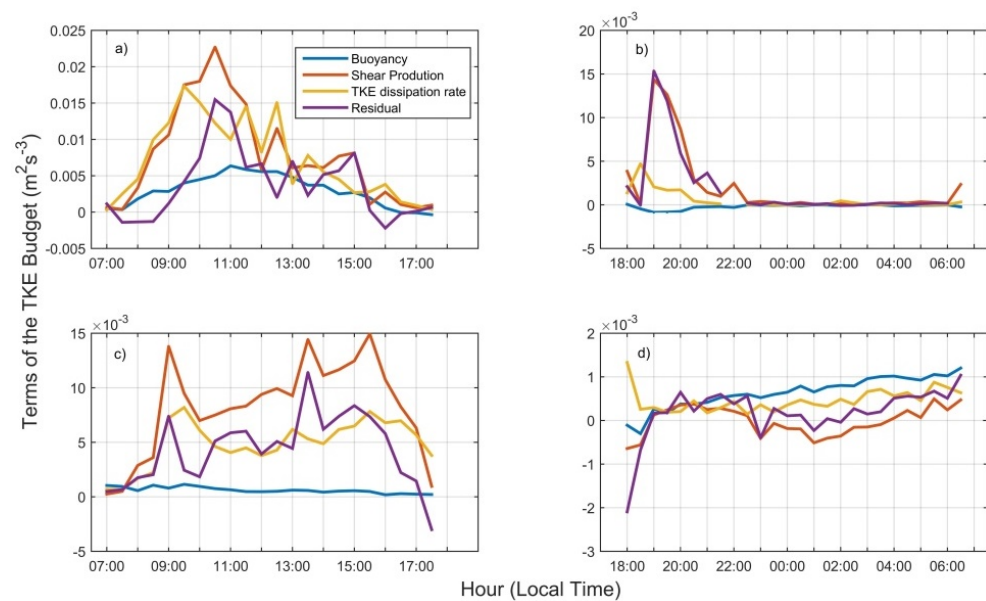


Figure 7. Diurnal cycle of the terms of the TKE budget for the K34 ((a,b) for daytime and nighttime, respectively) and CU ((c,d) for daytime and nighttime, respectively) sites.

Comparing the shear production during the diurnal period at each site, the curves of these variables are closer to each other in the forest than in the lake. This result shows that a surface that is efficient in “generating” turbulence is also efficient in dissipating it [15,44].

During the night at the k34 site (Figure 7b) the shear production and curves were very close to zero, except during 19 LT, where there is a prominent peak in shear production. This peak is a result of intermittent turbulence bursts which, curiously, occurred preferentially early in the night at the forest. On the other hand, turbulence over the lake is continuous and maintained by the buoyancy term in the TKE budget equation.

4. Conclusions

In this work the characteristics of the atmospheric turbulence on a smooth surface (lake) and a rough surface (forest) were compared. At each site turbulence intensity, temporal and length scales of the largest eddies, turbulence power spectra, as well as the main terms of the TKE budget (TKE = turbulent kinetic energy) were measured. During the daytime the turbulence intensity above the forest was greater than above the lake. The σ_w values calculated for the forest were approximately twice as high as those calculated for the lake, close to mid-day. In the nighttime period the situation was reversed, and the turbulence above the lake was practically continuous, with higher values of σ_w than the forest, except for periods in which intermittent turbulence bursts occur in K34. These bursts occurred primarily in the early evening on the days studied here.

The time and length scale of the largest eddies in the horizontal and vertical directions were calculated. The values obtained for the forest were close to those found in the literature for this surface, for example, the values of L_u and L_w were related to canopy height ($L_u = 35.2$, $L_w = 11.1$ and $h = 35$ m), as indicated by [43]. The scales obtained for the lake were probably the first on this surface in tropical regions. These scales had lower values than at the forest, except for the horizontal length scale ($L_u = 48.0$ m, above the lake).

The composites of the w power spectra showed a very similar behavior to the canonical ones above the lake. The region of the inertial subdomain with decay of $-5/3$ appears in both in day and nighttime periods above this surface. Above the forest this spectrum is well defined only during the daytime. In the nighttime period spectrums obtained during the performance of weak winds, below 1 ms^{-1} , contributed to the deformation of the spectrum in the region of medium frequency.

The buoyancy, shear production and TKE dissipation rate (ϵ), which are terms of the TKE budget equation, were calculated. Shear production was the term that most contributed to the generation of turbulence on both surfaces during the daytime. In the forest the buoyancy values were comparable to those of shear production from 12 to 16 h (local time). On the other hand, at the lake, the buoyancy values were very close to zero during the whole diurnal cycle. The behavior of ϵ follows the same trend as shear production. All terms calculated in this work had values very close to zero on the lake at night, indicating that other terms that could not be calculated, such as TKE advection, may have contributed to the turbulence overnight at this site.

Author Contributions: Conceptualization, R.A.S.S., C.Q.D.-J. and J.T.; Data curation, R.T.; Formal analysis, R.A.S.S. and R.d.S.; Methodology, R.A.S.S., C.Q.D.-J. and R.S.d.V.; Supervision, A.O.M.; Writing—original draft, R.A.S.S., T.P.B. and C.Q.D.-J.; writing—review and editing, R.A.S.S. and C.Q.D.-J. All authors have read and agreed to the published version of the manuscript.

Funding: This research received no external funding.

Institutional Review Board Statement: Not applicable.

Informed Consent Statement: Not applicable.

Data Availability Statement: Not applicable.

Acknowledgments: The authors are grateful to Daniel Jati for the preparation of Figure 1 of this paper, as well as for help in assembling the floating buoy experiment at the Curuá-Una site. The first author thanks the Coordenação de Aperfeiçoamento de Pessoal de Nível Superior (CAPES) for the PhD grant awarded through the Programa de Pos-graduação em Clima e Ambiente and the Universidade Federal do Oeste do Pará (UFOPA) for the partial release (20 h a week), which allowed for the accomplishment of this work. The authors also thank these institutions for their financial and logistical support in obtaining data on Lake Curuá-Una. The authors would like to thank all the development and teaching and research institutions that provided financial and human resources to obtain the data at the k34 site, namely: Fundação de Amparo a Pesquisa do Estado do Amazonas (FAPEAM), Fundação de Amparo a Pesquisa do Estado de São Paulo (FAPESP), Universidade do Estado do Amazonas (UEA), Instituto Nacional de Pesquisas da Amazônia (INPA) and the Programa de Grande Escala da Biosfera-Atmosfera na Amazônia (LBA). The authors also would like to thank the Centrais Elétricas do Norte do Brasil S.A (Eletronorte) for all operational support.

Conflicts of Interest: The authors declare no conflict of interest.

References

1. Garratt, J. *The Atmospheric Boundary Layer*; Cambridge University Press: Cambridge, UK, 1994; pp. 316–335.
2. Richey, J.E.; Melack, J.M.; Aufdenkampe, A.K.; Ballester, V.M.; Hess, L.L. Outgassing from Amazonian rivers and wetlands as a large tropical source of atmospheric CO₂. *Nature* **2002**, *416*, 617. [[CrossRef](#)]
3. Fisch, G.; Tota, J.; Machado, L.A.T.; Silva Dias, M.A.F.; da Lyra, R.F.F.; Nobre, C.A.; Dolman, A.J.; Gash, J.H.C. The convective boundary layer over pasture and forest in Amazonia. *Theor. Appl. Climatol.* **2004**, *78*, 47–59. [[CrossRef](#)]
4. Von Randow, C.; Zeri, M.; Restrepo-Coupe, N.; Muza, M.N.; de Gonçalves, L.G.G.; Costa, M.H.; Araujo, A.C.; Manzi, A.O.; da Rocha, H.R.; Saleska, S.R.; et al. Inter-annual variability of carbon and water fluxes in Amazonian forest, Cerrado and pasture sites, as simulated by terrestrial biosphere models. *Agric. For. Meteorol.* **2013**, *182–183*, 145–155. [[CrossRef](#)]
5. Arya, P.S. *Introduction to Micrometeorology*; Elsevier: Amsterdam, The Netherlands, 2001; Volume 79.
6. Kaimal, J.C.; Wyngaard, J.C. The Kansas and Minnesota experiments. *Bound. Layer Meteorol.* **1990**, *50*, 31–47. [[CrossRef](#)]
7. Fitzjarrald, D.R.; Moore, K.E.; Cabral, O.M.R.; Scolar, J.; Manzi, A.O.; de Abreu Sá, L.D. Daytime turbulent exchange between the Amazon forest and the atmosphere. *J. Geophys. Res. Atmos.* **1990**, *95*, 16825–16838. [[CrossRef](#)]
8. Kruijft, B.; Malhi, Y.; Lloyd, J.; Nobre, A.D.; Miranda, A.C.; Pereira, M.G.P.; Culf, A.; Grace, J. Turbulence Statistics Above and Within Two Amazon Rain Forest Canopies. *Bound. Layer Meteorol.* **2000**, *94*, 297–331. [[CrossRef](#)]
9. Santos, D.M.; Acevedo, O.C.; Chamecki, M.; Fuentes, J.D.; Gerken, T.; Stoy, P.C. Temporal Scales of the Nocturnal Flow Within and Above a Forest Canopy in Amazonia. *Bound. Layer Meteorol.* **2016**, *161*, 73–98. [[CrossRef](#)]
10. Dias-Júnior, C.Q.; Sá, L.D.; Filho, E.P.M.; Santana, R.A.; Mauder, M.; Manzi, A.O. Turbulence regimes in the stable boundary layer above and within the Amazon forest. *Agric. For. Meteorol.* **2017**, *233*, 122–132. [[CrossRef](#)]
11. Freire, L.S.; Gerken, T.; Ruiz-Plancarte, J.; Wei, D.; Fuentes, J.D.; Katul, G.G.; Dias, N.L.; Acevedo, O.C.; Chamecki, M. Turbulent mixing and removal of ozone within an Amazon rainforest canopy. *J. Geophys. Res. Atmos.* **2017**, *122*, 2791–2811. [[CrossRef](#)]

12. Dias-Júnior, C.Q.; Dias, N.L.; dos Santos, R.M.N.; Sörgel, M.; Araújo, A.; Tsokankunku, A.; Ditas, F.; de Santana, R.A.; Von Randow, C.; Sá, M.; et al. Is there a classical inertial sublayer over the Amazon forest? *Geophys. Res. Lett.* **2019**, *46*, 5614–5622. [[CrossRef](#)]
13. Chamecki, M.; Freire, L.S.; Dias, N.L.; Chen, B.; Dias-Junior, C.Q.; Toledo Machado, L.A.; Sörgel, M.; Tsokankunku, A.; Araújo, A.C.D. Effects of vegetation and topography on the boundary layer structure above the Amazon forest. *J. Atmos. Sci.* **2020**, *77*, 2941–2957. [[CrossRef](#)]
14. Vale, R.S. *Medições de Gases de Efeito Estufa e Variáveis Ambientais em Reservatórios Hidrelétricos na Amazônia Central*. Ph.D. Thesis, Instituto Nacional de Pesquisas da Amazônia, Manaus, Spain, 2016.
15. Stull, R.B. *An Introduction to Boundary Layer Meteorology*; Springer: Dordrecht, The Netherlands, 1988.
16. Kundu, P.K.; Cohen, I.M. *Fluid Mechanics*; Academic Press: San Diego, CA, USA, 2002.
17. Kaimal, J.C.; Finnigan, J.J. *Atmospheric Boundary Layer Flows: Their Structure and Measurement*; Oxford University Press: New York, NY, USA, 1994.
18. Anderson, D.E.; Verma, S.B.; Clement, R.J.; Baldocchi, D.D.; Matt, D.R. Turbulence spectra of CO₂, water vapor, temperature and velocity over a deciduous forest. *Agric. For. Meteorol.* **1986**, *38*, 81–99. [[CrossRef](#)]
19. Lee, X. Turbulence spectra and eddy diffusivity over forests. *J. Appl. Meteorol.* **1996**, *35*, 1307–1318. [[CrossRef](#)]
20. Moraes, O.L.; Fitzjarrald, D.R.; Acevedo, O.C.; Sakai, R.K.; Czirkowsky, M.J.; Degrazia, G.A. Comparing spectra and cospectra of turbulence over different surface boundary conditions. *Phys. A Stat. Mech. Its Appl.* **2008**, *387*, 4927–4939. [[CrossRef](#)]
21. Sahlée, E.; Rutgersson, A.; Podgrajsek, E.; Bergström, H. Influence from surrounding land on the turbulence measurements above a lake. *Bound. Layer Meteorol.* **2014**, *150*, 235–258. [[CrossRef](#)]
22. Kaimal, J.C.; Wyngaard, J.C.; Izumi, Y.; Côté, O.R. Spectral characteristics of surface-layer turbulence. *Q. J. R. Meteorol. Soc.* **1972**, *98*, 563–589. [[CrossRef](#)]
23. Walter, R.K.; Nidzieko, N.J.; Monismith, S.G. Similarity scaling of turbulence spectra and cospectra in a shallow tidal flow. *J. Geophys. Res. Ocean.* **2011**, *116*. [[CrossRef](#)]
24. Araújo, A.C.; Nobre, A.D.; Kruijt, B.; Elbers, J.A.; Dallarosa, R.; Stefani, P.; von Randow, C.; Manzi, A.O.; Culf, A.D.; Gash, J.H.C.; et al. Comparative measurements of carbon dioxide fluxes from two nearby towers in a central Amazonian rainforest: The Manaus LBA site. *J. Geophys. Res. Atmos.* **2002**, *107*. [[CrossRef](#)]
25. Fearnside, P.M. Do hydroelectric dams mitigate global warming? The case of Brazil's Curuá-Una Dam. *Mitig. Adapt. Strateg. Glob. Chang.* **2005**, *10*, 675–691. [[CrossRef](#)]
26. Fuentes, J.D.; Chamecki, M.; dos Santos, R.M.N.; Randow, C.V.; Stoy, P.C.; Katul, G.; Fitzjarrald, D.; Manzi, A.; Gerken, T.; Trowbridge, A.; et al. Linking Meteorology, Turbulence, and Air Chemistry in the Amazon Rain Forest. *Bull. Am. Meteorol. Soc.* **2016**, *97*, 2329–2342. [[CrossRef](#)]
27. Wilczak, J.M.; Oncley, S.P.; Stage, S.A. Sonic anemometer tilt correction algorithms. *Bound. Layer Meteorol.* **2001**, *99*, 127–150. [[CrossRef](#)]
28. Vickers, D.; Mahrt, L. Quality Control and Flux Sampling Problems for Tower and Aircraft Data. *J. Atmos. Ocean. Technol.* **1997**, *14*, 512–526. [[CrossRef](#)]
29. Mahrt, L.; Lee, X.; Black, A.; Neumann, H.; Staebler, R. Nocturnal mixing in a forest subcanopy. *Agric. For. Meteorol.* **2000**, *101*, 67–78. [[CrossRef](#)]
30. Fitzjarrald, D.R.; Stormwind, B.L.; Fisch, G.; Cabral, O.M.R. Turbulent transport observed just above the Amazon forest. *J. Geophys. Res. Atmos.* **1988**, *93*, 1551–1563. [[CrossRef](#)]
31. Santana, R.A.; Dias-Júnior, C.Q.; Tóta, J.; Fuentes, J.D.; do Vale, R.S.; Alves, E.G.; dos Santos, R.M.N.; Manzi, A.O. Air turbulence characteristics at multiple sites in and above the Amazon rainforest canopy. *Agric. For. Meteorol.* **2018**, *260–261*, 41–54. [[CrossRef](#)]
32. Acevedo, O.C.; Fitzjarrald, D.R. In the Core of the Night-Effects of Intermittent Mixing on a Horizontally Heterogeneous Surface. *Bound. Layer Meteorol.* **2003**, *106*, 1–33. [[CrossRef](#)]
33. Oliveira, P.E.; Acevedo, O.C.; Moraes, O.L.; Zimmermann, H.R.; Teichrieb, C. Nocturnal intermittent coupling between the interior of a pine forest and the air above it. *Bound. Layer Meteorol.* **2013**, *146*, 45–64. [[CrossRef](#)]
34. De Oliveira, F.P.; Oyama, M.D. Antecedent Atmospheric Conditions Related to Squall-Line Initiation over the Northern Coast of Brazil in July. *Weather Forecast.* **2015**, *30*, 1254–1264. [[CrossRef](#)]
35. Yi, C. Momentum transfer within canopies. *J. Appl. Meteorol. Climatol.* **2008**, *47*, 262–275. [[CrossRef](#)]
36. De Souza, C.M.; Dias-Júnior, C.Q.; Tóta, J.; de Abreu Sá, L.D. An empirical-analytical model of the vertical wind speed profile above and within an Amazon forest site. *Meteorol. Appl.* **2016**, *23*, 158–164. [[CrossRef](#)]
37. Santana, R.A.S.D.; Dias-Júnior, C.Q.; Vale, R.S.D.; Tóta, J.; Fitzjarrald, D.R. Observing and Modeling the Vertical Wind Profile at Multiple Sites in and above the Amazon Rain Forest Canopy. *Adv. Meteorol.* **2017**, *2017*, 5436157. [[CrossRef](#)]
38. Poggi, D.; Porporato, A.; Ridolfi, L.; Albertson, J.D.; Katul, G.G. The Effect of Vegetation Density on Canopy Sub-Layer Turbulence. *Bound. Layer Meteorol.* **2004**, *111*, 565–587. [[CrossRef](#)]
39. Malhi, Y.; Pegoraro, E.; Nobre, A.D.; Pereira, M.G.P.; Grace, J.; Culf, A.D.; Clement, R. Energy and water dynamics of a central Amazonian rain forest. *J. Geophys. Res. Atmos.* **2002**, *107*, LBA 45-1–LBA 45-17. [[CrossRef](#)]
40. Lumley, J.L.; Panofsky, H.A. *The Structure of Atmospheric Turbulence*; John Wiley & Sons: New York, NY, USA, 1964.
41. Shaw, R.; Brunet, Y.; Finnigan, J.; Raupach, M. A wind tunnel study of air flow in waving wheat: Two-point velocity statistics. *Bound. Layer Meteorol.* **1995**, *76*, 349–376. [[CrossRef](#)]

42. Vesala, T.; Eugster, W.; Ojala, A. *Eddy Covariance—A Practical Guide to Measurement and Data Analysis*; Eddy Covariance Measurements over Lake Fluxes; Springer Atmospheric Sciences: Berlin/Heidelberg, Germany, 2012; pp. 335–375.
43. Raupach, M.R.; Finnigan, J.J.; Brunei, Y. Coherent eddies and turbulence in vegetation canopies: The mixing-layer analogy. *Bound. Layer Meteorol.* **1996**, *78*, 351–382. [[CrossRef](#)]
44. Bezerra, V.L.; Dias-Júnior, C.Q.; Vale, R.S.; Santana, R.A.; Botía, S.; Manzi, A.O.; Cohen, J.C.; Martins, H.S.; Chamecki, M.; Fuentes, J.D. Near-surface atmospheric turbulence in the presence of a squall line above a forested and deforested region in the central amazon. *Atmosphere* **2021**, *12*, 461. [[CrossRef](#)]